“A Unified Computational Model for Solar and Stellar Flares” by Allred et al. (2015)

Natsuha Kuroda

NJIT/CSTR weekly group meeting

10/01/2015

Introduction

- Simulate the transport of a beam of non-thermal particles injected at the top of a magnetic flux tube which extends from sub-photosphere to the corona
- Requires a computation grid with < 100m
- Currently, only in 1D
- Includes the effects of accelerated ions and return current

The equations of radiation hydrodynamics (RADYN code)

$$\frac{\partial \rho}{\partial t} + \frac{\partial \rho v}{\partial z} = 0, \quad (1)$$

$$\frac{\partial \rho v}{\partial t} + \frac{\partial \rho v^2}{\partial z} + \frac{\partial (p + q_v)}{\partial z} + \rho g - A_{\text{beam}} = 0, \quad (2)$$

$$\frac{\partial \rho e}{\partial t} + \frac{\partial \rho v e}{\partial z} + (p + q_v)\frac{\partial v}{\partial z} + \frac{\partial (F_c + F_r)}{\partial z} - Q_{\text{cor}} - Q_{\text{beam}} - Q_{\text{rc}} = 0, \quad (3)$$

$$\frac{\partial n_i}{\partial t} + \frac{\partial n_i v}{\partial z} - \left(\sum_{j \neq i}^{N'} n_j P_{ji} - n_i \sum_{j \neq i}^{N'} P_{ij} \right) = 0, \quad (4)$$

$$\mu \frac{\partial I_{\nu\mu}}{\partial z} = \eta_{\nu\mu} - \chi_{\nu\mu} I_{\nu\mu} \quad (5)$$

- z = height
- ρ = density
- e = internal energy density
- v = velocity
- p = pressure
- $F_{c/r}$ = conductive/radiative flux
- n_i = number density in a given atomic state
- N’ = total number of atomic states
- P_{ij} = transition rate from state i to state j
- $\eta_{\nu\mu}$ = emission coefficient
- $\chi_{\nu\mu}$ = absorption coefficient
- Q_{cor} = coronal heating term
- Q_{beam} = flare-accelerated particle beam heating
- A_{beam} = flare-accelerated particle beam momentum deposition
- Q_{rc} = return current heating term

Optically thick radiative transfer (chromosphere)

Table 1
Bound–Bound Transitions

Atom	λ_{ij} (Å)[a]	Transition	Atom	λ_{ij} (Å)	Transition
H I	1215.67	Lyα	Ca II	8662.14	$3d\ ^2D_{3/2} \leftrightarrow 4p\ ^2P^o_{1/2}$
	1025.73	Lyβ	⋯	8498.02	$3d\ ^2D_{3/2} \leftrightarrow 4p\ ^2P^o_{3/2}$
	972.52	Lyγ	⋯	8542.09	$3d\ ^2D_{5/2} \leftrightarrow 4p\ ^2P^o_{3/2}$
	949.74	Lyδ	He I	625.56	$1s^2\ ^1S_0 \leftrightarrow 1s\ 2s\ ^3S_1$
	6562.79	Hα	⋯	601.42	$1s^2\ ^1S_0 \leftrightarrow 1s\ 2s\ ^1S_0$
	4861.35	Hβ	⋯	10830.29	$1s\ 2s\ ^3S_1 \leftrightarrow 1s\ 2p\ ^3P^0_4$
	4340.47	Hγ	⋯	584.33	$1s^2\ ^1S_0 \leftrightarrow 1s\ 2p\ ^1P^0_1$
	18751.3	Paα	⋯	20581.29	$1s\ 2s\ ^1S_0 \leftrightarrow 1s\ 2p\ ^1P^0_1$
	12818.1	Paβ	He II	303.79	$1s\ ^2S_{1/2} \leftrightarrow 1s\ 2p\ ^2S_{1/2}$
	40522.8	Brα	⋯	303.78	$1s\ ^2S_{1/2} \leftrightarrow 2p\ ^2P^0_2$
Ca II	3968.47				h
	3933.66				k

Table 2
Bound–Free Transitions

Atom	λ_{ic} (Å)	Initial State	Atom	λ_{ic} (Å)	Initial State
H I	911	$n = 1$	He I	504	$1s^2\ ^1S_0$
	3646	$n = 2$	⋯	2600	$1s\ 2s\ ^3S_1$
	8204	$n = 3$	⋯	3121	$1s\ 2s\ ^1S_0$
	14584	$n = 4$	⋯	3421	$1s\ 2p\ ^3P^0_4$
	22787	$n = 5$	⋯	3679	$1s\ 2p\ ^1P^0_1$
Ca II	1044	$4s\ ^2S_{1/2}$	He II	228	$1s\ ^2S_{1/2}$
	1218	$3d\ ^2D_{3/2}$	⋯	911	$2s\ ^2S_{1/2}$
	1219	$3d\ ^2D_{5/2}$	⋯	911	$2p\ ^2P^0_{1/2}$
	1417	$4p\ ^2P^o_{1/2}$	Mg II	824	$2p^6\ 3s\ ^2S_{1/2}$
	1422	$4p\ ^2P^o_{3/2}$	⋯	1168	$2p^6\ 4p\ ^2P^0_{1/2}$
	⋯	⋯	⋯	1169	$2p^6\ 4p\ ^2P^0_{3/2}$

Optically thin radiative transfer (transition region & corona)

- "Coronal approximation": optically thin & net cooling effect – radiative loss function
- Assumes a constant electron density of 10^{10} cm^{-3}

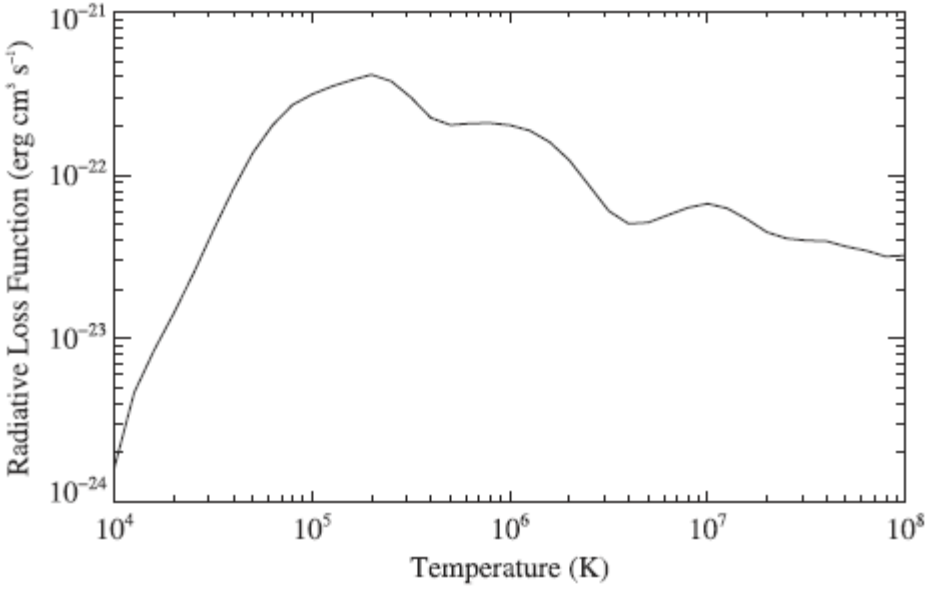

Figure 1. Optically thin radiative loss function used in these simulations.

XEUV backwarming

- "The other half" of the optically thin radiative loss
- Heating + ph

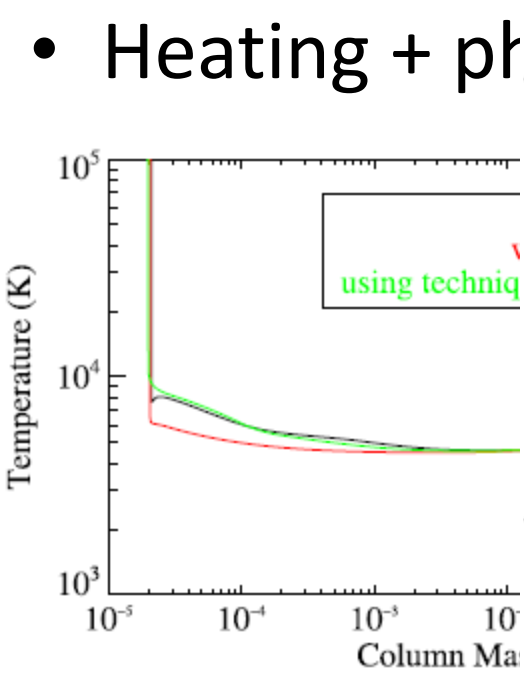

Figure 2. Temperature as a function of colu
using the XEUV backwarming method desc
technique of A05 (green), and without XE

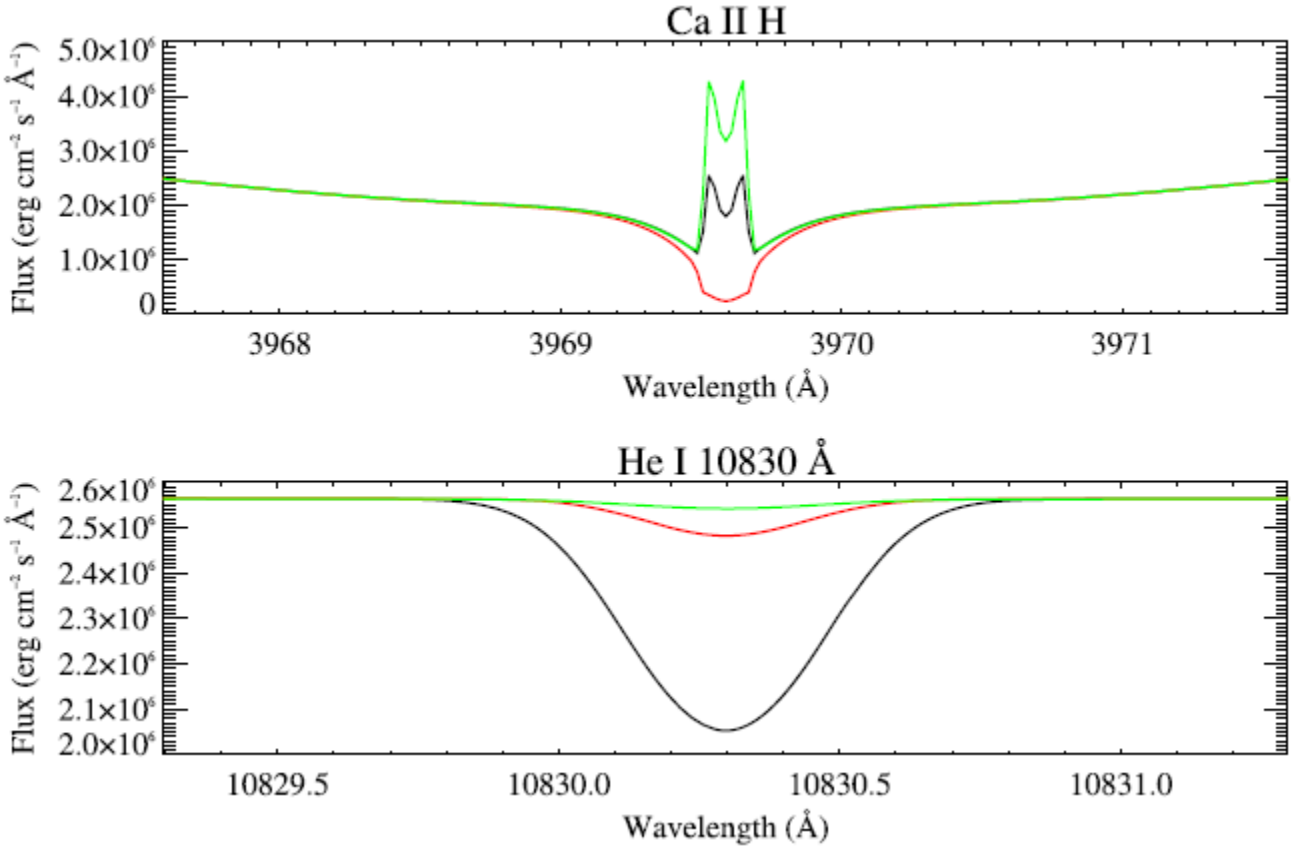

Line broadening

- Hydrogen Balmer lines can become extremely broadened during flares
- **Stark broadening** - the shifting and splitting of spectral lines of atoms and molecules due to presence of **an external electric field**

Initial loops

- 3 free parameters – photospheric temperature, loop-length, & coronal temperature
- B-fields: 1,000 G for solar photosphere, 100 G for the top of the shorter solar loops, & 10 G for the top of the larger solar loops

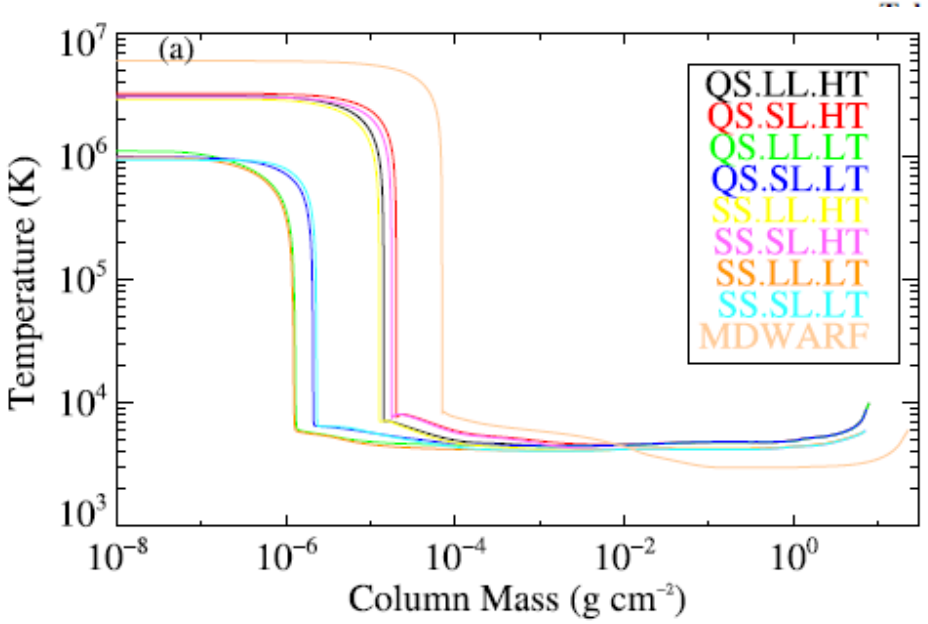

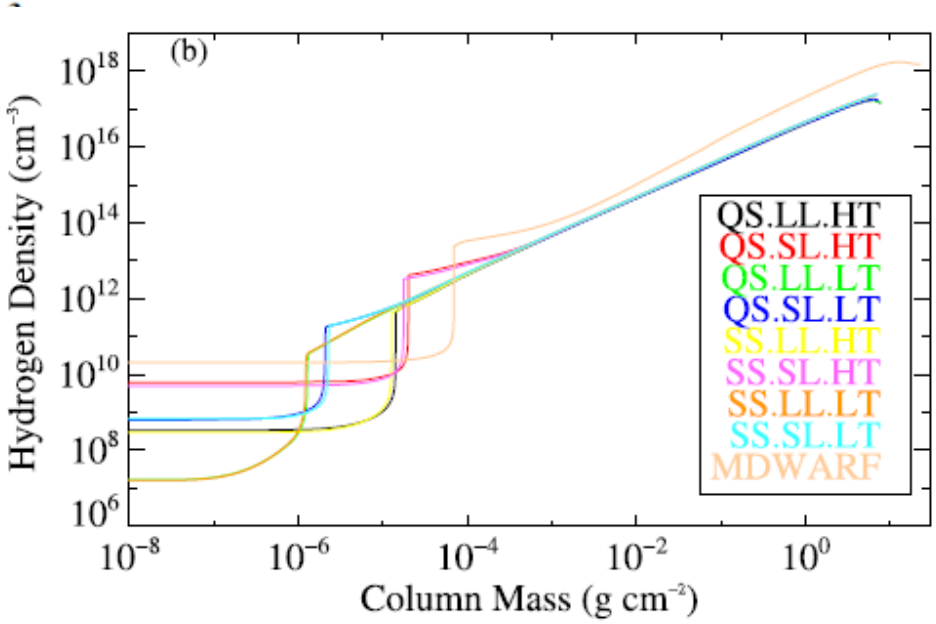

Particle beam heating (Q_{beam} & A_{beam})

- The rate of energy lost by a particle beam depends on

$$\mu\frac{\partial\Phi}{\partial z}-\frac{d\ln B}{2dz}\frac{\partial}{\partial\mu}\left[\left(1-\mu^2\right)\Phi\right]$$
$$=\frac{1}{\beta^2}\frac{\partial}{\partial E}\left\{\left[C+S\beta^3\gamma^2\left(1-\mu^2\right)\right]\Phi\right\}$$
$$-\frac{S}{\beta\gamma}\frac{\partial}{\partial\mu}\left[\mu\left(1-\mu^2\right)\Phi\right]$$
$$+\frac{C'}{\beta^4\gamma^2}\frac{\partial}{\partial\mu}\left[\left(1-\mu^2\right)\frac{\partial\Phi}{\partial\mu}\right]+\frac{\Sigma}{c\beta^2}$$

emission

- Σ = source term for particles injected at the loop top
- C/C’ = coefficients for the beam energy loss rate/pitch-angle diffusion from collisions
- S = coefficient for the loss rate and pitch-angle diffusion due to synchrotron emission

Particle beam heating (Q_{beam} & A_{beam})

- Consider a plasma consisting of electrons, protons, neutral hydrogen, neutral, singly and doubly ionized helium, and slightly ionized calcium and magnesium
- The beam energy deposition drives the simulations which alter the beam deposition in a self-consistent way

Particle beam collision rates (P_{ij})

- During flares, transition rates can be very enhanced due to direct ionizations and excitations caused by collisions of non-thermal particles with the ambient plasma
- Secondary ionizations from electrons liberated in the primary ionization is included

Return current (Q_{rc})

- Decelerates the beam electrons while accelerating ambient electrons, which drift in the direction opposite to that of the return current electric field toward the loop top
- Heats the atmosphere through Ohmic disspation

$$Q_{\mathrm{rc}}(x) = \begin{cases} \eta e^2 F_{\mathrm{e}}{}^2 & x < x_{\mathrm{rc}} \\ \eta e^2 F_{\mathrm{e}}{}^2 \left(\delta \dfrac{E_{\mathrm{therm}}}{E_{\mathrm{c}}} + \dfrac{V(x)}{E_{\mathrm{c}}} \right) & \\ \times \left(\dfrac{E_{\mathrm{therm}}}{E_{\mathrm{c}}} + \dfrac{V(x)}{E_{\mathrm{c}}} \right)^{1-2\delta} & x \geqslant x_{\mathrm{rc}} \end{cases}$$

- x = distance from the loop top
- F_e = beam particle flux
- δ = power-law index
- E_c = cutoff energy

Parameter study

- Varying the injected **electron beam spectrum**, **pitch-angle distribution**, and **the initial loop conditions** into which the particles impact

Table 4
Parameter Study

Parameter	Range
E_c	5–500 keV
δ	2.5–10
μ_0	0.1–1.0, isotropic, beamed
Loop Conditions	Those listed in Table 3

Table 3
Initial Loops

Label	Photospheric Temperature (K)	Loop-length (Mm)	Coronal Electron Density (cm^{-3})	Coronal Temperature (MK)
QS.LL.HT	5800	100	3×10^8	3.0
QS.LL.LT	5800	100	2×10^7	1.0
QS.SL.HT	5800	10	6×10^9	3.0
QS.SL.LT	5800	10	6×10^8	1.0
SS.LL.HT	5000	100	3×10^8	3.0
SS.LL.LT	5000	100	2×10^7	1.0
SS.SL.HT	5000	10	6×10^9	3.0
SS.SL.LT	5000	10	6×10^8	1.0
M dwarf	3500	10	2×10^{10}	6.0

Penetration depths in flux loops – varying E_c and δ

- Penetration depth is **strongly dependent on δ**
- As the cutoff energy increases, **relativistic effects** become significant (right panel)

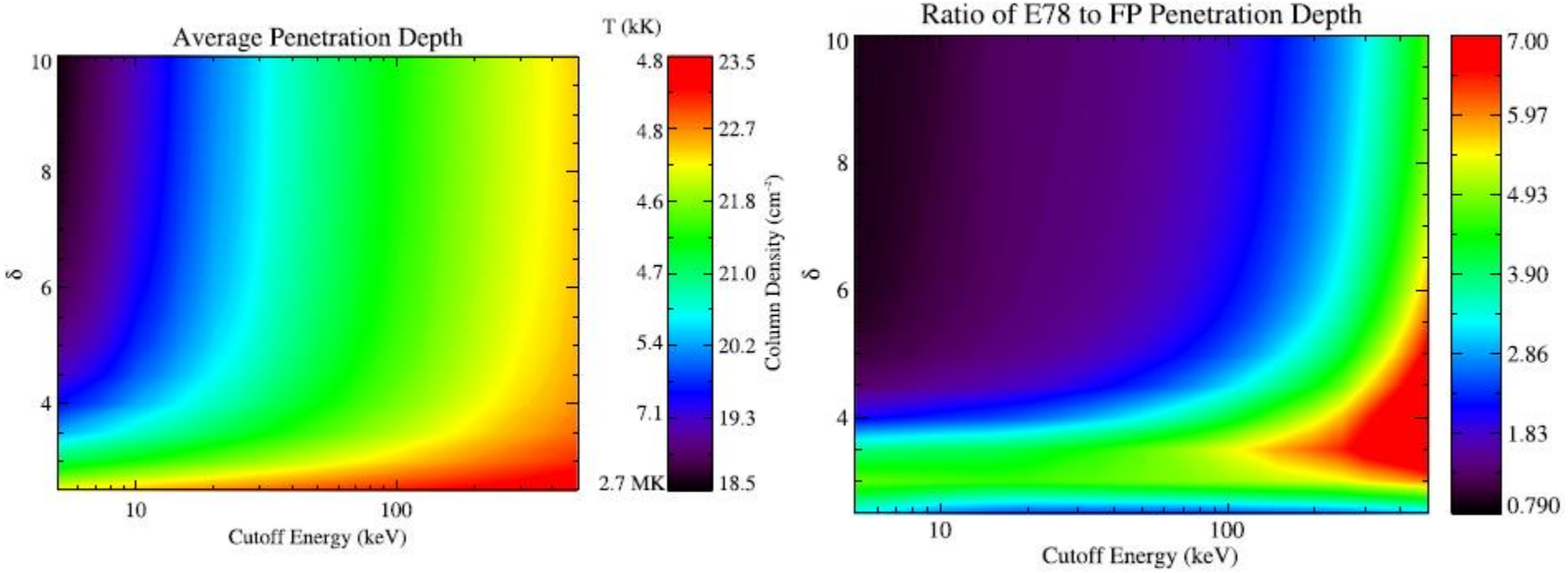

Penetration depths in flux loops – for several kinds of loops

- For **low values of E_c**, the beam penetrates **more deeply** in **a low temperature loop**, but **less deeply** in **a shorter loop**

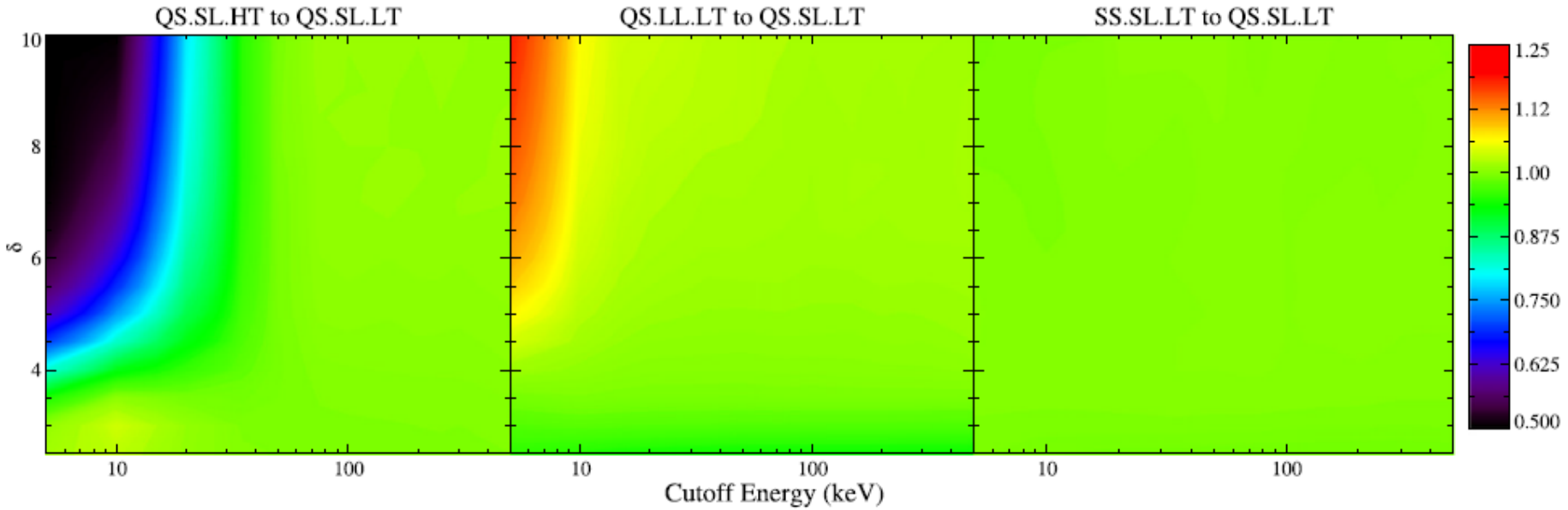

Figure 9. Ratio of the beam penetration depth in the QS.SL.HT (left), QS.LL.LT (middle), and SS.SL.LT (right) atmospheres to the penetration depth in the QS.SL.LT simulation as a function of cutoff energy and spectral index.

Penetration depths in flux loops – pitch-angle distribution

- **The beamed electrons** penetrate **more deeply**

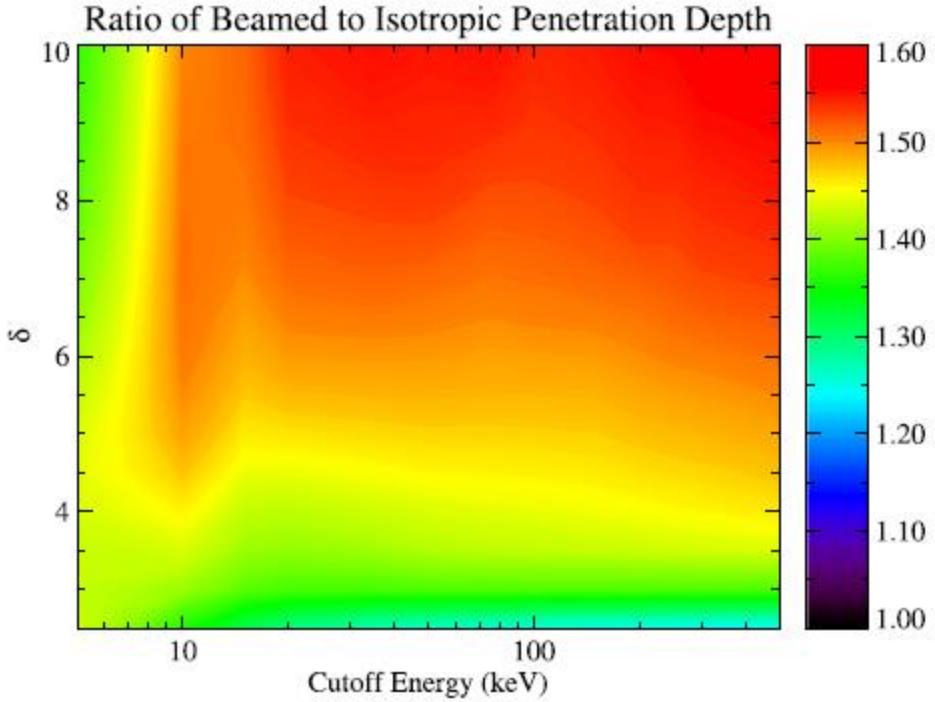

Figure 8. Ratio of the penetration depth for a highly beamed to isotropic injected distribution. Calculated using the QS.SL.HT initial atmosphere.

Collision rates – for different loops

- The ionization rates increase dramatically **around beam impact**
- Relatively **independent** of **the initial loop conditions**

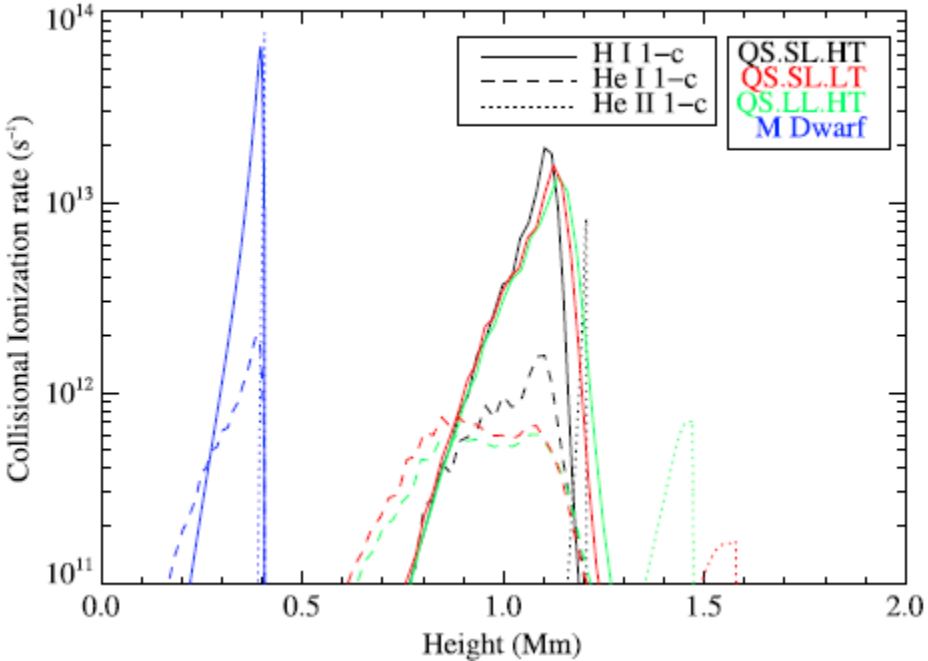

Collision rates – varying E_c and δ

- Ionization rates peak at **lower E_c** and **higher δ** (Q_{beam} peak)
- He II – a beam with **larger E_c** penetrates to **a deeper, cooler region**, where He II density is **lower**

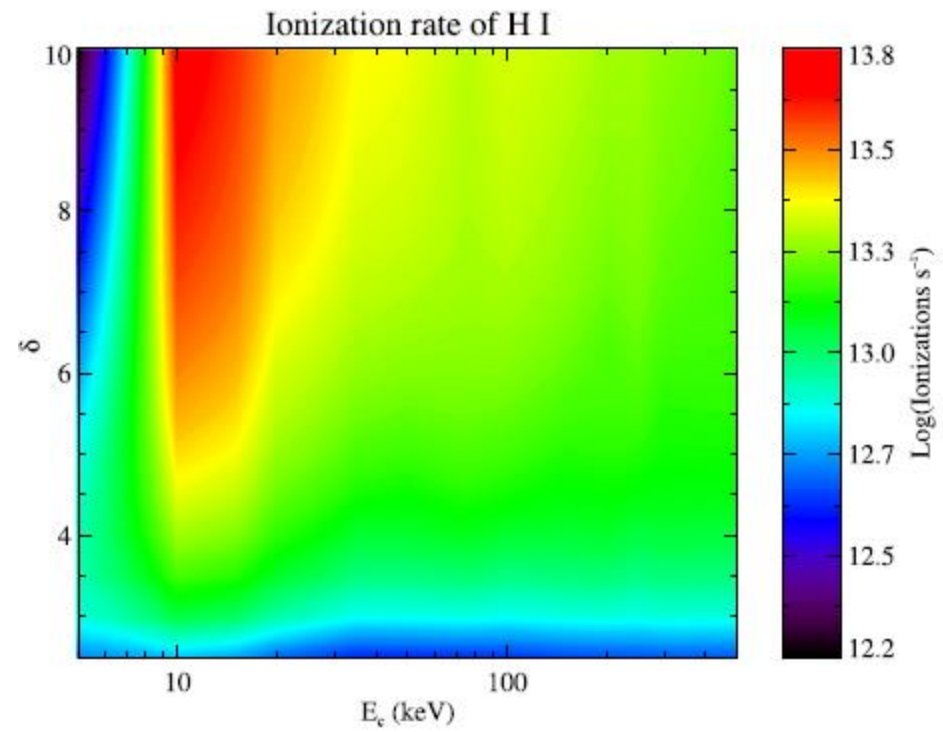

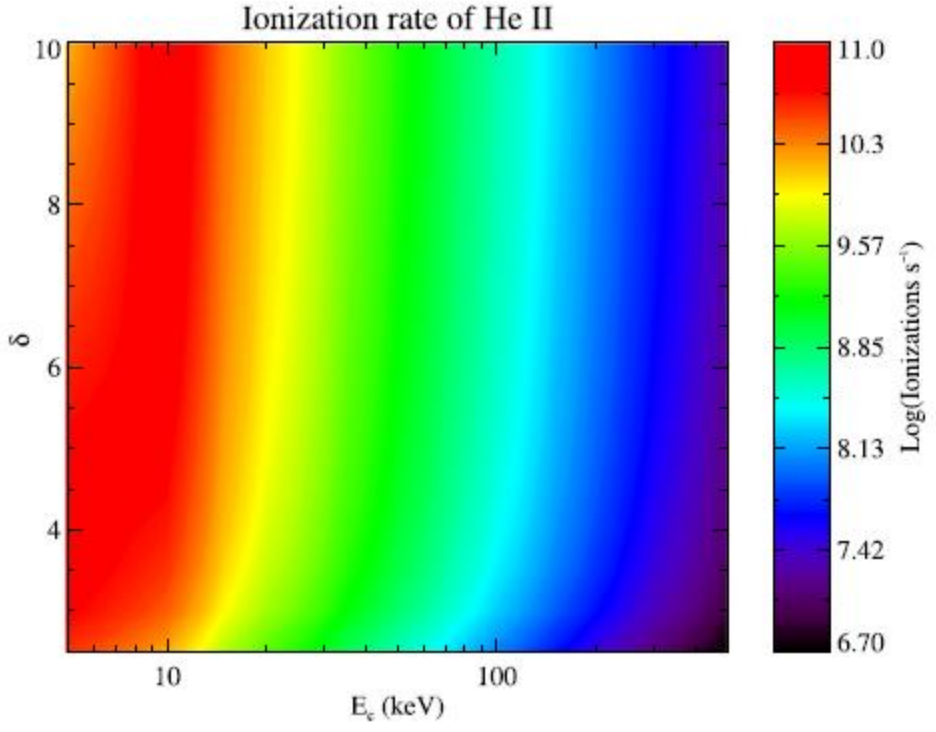

Return current heating **in the corona**

- In most cases, **Q_{rc} dominates**, being **stronger** in **the cooler loop**
- Pitch-angle distribution makes **little difference** in Q_{rc}
- Return currents are likely to be most important in **the early phases of flares** before the corona has been heated to very high temperature

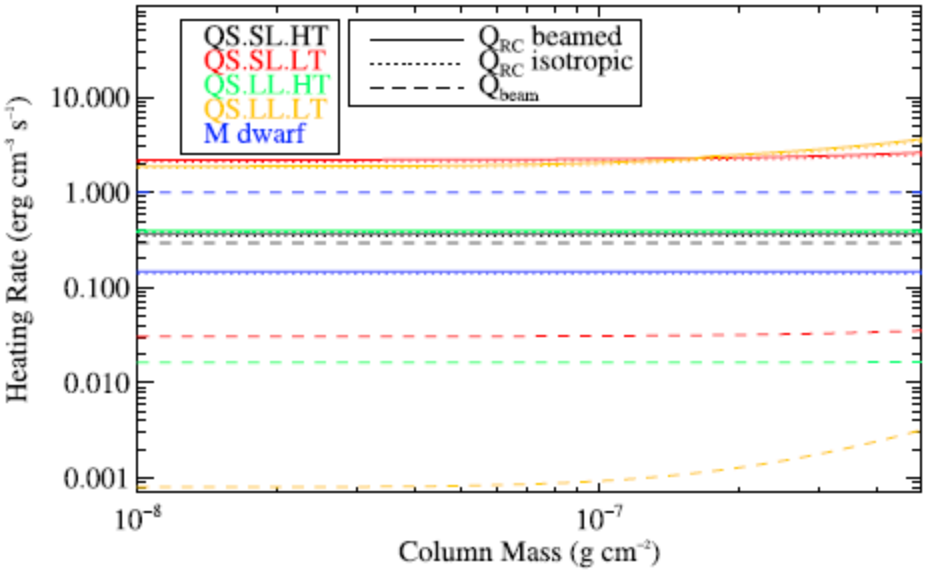

Conclusions

- The penetration depth of the particles with a power-law energy distribution is strongly dependent on **E_c and δ**, but is weakly dependent on their initial pitch-angle distribution
- For distributions with **low δ** or **high E_c**, penetration depth is **much less than predicted by classical theory** due to **relativistic effect**
- Varying **the condition of the loops** has **small effects** on the penetration depth for distributions with **low E_c**
- **The collisional rates** are also strongly dependent on **E_c and δ**
- Depending on coronal conditions, return current heating in the corona can be **much greater** than coronal beam heating

Reference

- Allred, J. C., Kowalski, A. F., & Carlsson, M. 2015, ApJ, 809, 104